ELSEVIER

Biochimica et Biophysica Acta 1321 (1997) 183–193

BIOCHIMICA ET BIOPHYSICA ACTA
BBA

Morphological and molecular changes in the unicellular green alga *Dunaliella salina* grown under supplemental UV-B radiation: cell characteristics and Photosystem II damage and repair properties

Antonio Masi [1], Anastasios Melis *

Plant and Microbial Biology, 411 Koshland Hall, University of California, Berkeley CA 94720-3102, USA

Received 12 March 1997; accepted 20 May 1997

Abstract

The effect of supplemental UV-B radiation during growth in the green alga *Dunaliella salina* was investigated. At the cellular level, supplemental UV-B radiation induced a doubling of the cell volume, a phenomenon attributed to a slow-down in the rate of cell division. At the thylakoid mebrane level, supplemetal UV-B radiation induced photodamage to the 32 kDa (D1) and 34 kDa (D2) reaction center proteins of Photosystem II. The molecular target of photodamage to D1 and D2, and the temporal sequence of events leading to repair of Photosystem II from this UV-B photodamage, appeared to be different from those that operate under photosynthetically active radiation (PAR). Thus, mechanistically, photodamage and repair under supplemental UV-B may be a distinctly different phenomenon from the damage and repair cycle induced by visible light. © 1997 Elsevier Science B.V.

Keywords: Photosynthesis; UV-B radiation; Photodamage; Photosystem II; Reaction center; 160 kDa complex; (*Dunaliella salina*)

1. Introduction

Light quality and light intensity exert significant effects on the organisation of the photosynthetic apparatus. Changes in the quality of photosynthetically active radiation (PAR) are known to bring about adjustment and optimisation in the relative concentration of Photosystems I and II in such diverse organisms as cyanophytes [1–3] red and green algae [4–6] and higher plant chloroplasts [7–9].

The level of irradiance during plant growth modulates the size and composition of the light-harvesting antenna of the photosystems [10,11]. In general, low light intensity promotes larger Chl antenna size for both PS I and PS II (larger photosynthetic unit size). High-light conditions elicit a smaller Chl antenna size. This adjustment in the Chl antenna size of the photosystems comes about because of changes in the size of the auxiliary Chl *ab* light-harvesting complex [12–15]. Persistently high levels of irradiance cause impairment in the activity of PS II and result in losses in the capacity for photosynthesis. This light-induced inhibition of photosynthesis is better known as *photoinhibition* [16]. The molecular basis of photoinhibition is photo-oxidative damage to the PS

Abbreviations: Chl, chlorophyll; PS II, Photosystem II; LHC, light-harvesting complex; Q_A, primary electron-accepting plastoquinone of Photosystem II; Q_B, secondary electron-accepting plastoquinone of Photosystem II

* Corresponding author. Fax: +1 (510) 642-4995; E-mail: melis@nature.berkeley.edu

[1] Permanent address: Dipartimento di Biotecnologie Agrarie, Strada Romea 16, 35020 Legnaro (PD), Italy. E-mail: masiman@agripolis.unipd.it

PII S0005-2728(97)00054-6

II reaction center [17–19]. This photodamage causes irreversible inactivation in the function of the 32 kDa (D1) reaction center protein and stops photosynthesis [20]. Under physiological conditions, photosynthesis recovers from this adverse effect through a repair process that restores the functional status of PS II. A central aspect of the PS II repair is the selective degradation [21] and turnover of the D1 protein [22,23]. This PS II damage and repair cycle, as the phenomenon has come to be known [24], is of great importance for the maintenance and productivity of photosynthesis.

A special case of irradiance-induced photodamage in plants is by supplemental UV-B radiation. The latter is known to bring about multiple adverse effects on photosynthesis: it lowers the quantum efficiency of photosynthesis, inhibits the electron transport and photophosphorylation processes, lowers the chloroplast protein content of Rubisco [25–27], and damages nucleic acids with a concomitant adverse effect on protein biosynthesis [28,29].

A combination of PAR and UV-B radiation results in enhanced rates of photodamage and degradation of the D1 protein [30], although UV-B driven protein cleavage occurs at different sites as compared to that induced by PAR, and is thought to be independent of the presence of oxygen [31–33]. It is further thought that different photosensitizers mediate D1 photodamage and degradation in the visible and UV-B spectral region [30,34].

The interplay between PAR and supplemental UV-B radiation and the role of the latter in photodamage and turnover of the D2 protein are questions of current interest. In this work, we addressed the effect of supplemental UV-B radiation on the morphology, growth and photodamage to D1 and D2 proteins in the green alga *Dunaliella salina* under in vivo conditions. The results show distinct effects at the cellular level and suggest independent adverse effects by PAR and UV-B on the photosynthetic apparatus.

2. Materials and methods

2.1. Cell growth

Dunaliella salina cells were grown in an artificial hypersaline medium similar to that of [35], containing 1.5 M NaCl, 5 mM $MgSO_4$, 0.3 mM $CaCl_2$, 0.1 mM KH_2PO_4, 20 μM EDTA, and 5 mM NH_4Cl supplemented with a mixture of iron and micronutrients. Carbon was supplied as $NaHCO_3$ at an initial concentration of 25 mM. Cells were cultivated in Petri dishes having a 6 cm radius and containing 40 ml culture medium so as to prevent shading and to allow for a uniform exposure of cells to photosynthetic and UV-B radiation. Mild agitation of the cell culture was achieved by placing the Petri dishes on an orbital shaker (Red Rotor, Hoefer Scientific) operated at a low speed. This configuration permitted a uniform illumination of cells and, at the same time, removal of O_2 from the liquid medium. The density of cells in the culture medium was counted using the Neubauer ultraplane and an Olympus BH-2 light microscope.

The *D. salina* culture was illuminated by a mixture of continuous incandescent and cool-white fluorescent light bulbs. The incident irradiance was 170–180 $\mu mol\ photons \cdot m^{-2} \cdot s^{-1}$, measured with a LICOR model LI-185B Quantum-Radiometer-Photometer connected to a LI-190SB sensor. UV-B radiation was provided by ultraviolet emitting fluorescent tubes (Philips model TL12/40W). The undesired short wavelength emission of these lamps in the UV-C region of the spectrum was filtered by screening through pre-solarized sheets of cellulose diacetate (absolute cut off at 280 nm). The incident intensity of the UV-B radiation at the level of the cell culture was 0.75 $\mu mol\ photons \cdot m^{-2} \cdot s^{-1}$, measured with a UV-B digital radiometer (UVP, model UVX).

2.2. Isolation of thylakoid membranes

D. salina cells in their mid-late logarithmic growth phase were harvested by centrifugation at $3000 \times g$ for 4 min at 4°C. Pellets were resuspended in 0.5 ml of fresh growth medium and stored frozen at −80°C until all samples were ready for processing. Samples were thawed on ice and diluted in 10 ml sonication buffer containing 100 mM Tris-HCl, 100 mM NaCl, 5 mM $MgCl_2$, 0.2% Na-ascorbate, 0.2% PVP, 1 mM 6-aminocaproic acid, 1 mM *p*-aminobenzamidine, pH 6.8. Cells were disrupted by sonication for 30 s in a Branson Sonifier operated in the pulsed mode with a 50% duty cycle and an output power setting of 5. Unbroken cells and other large cell fragments were

removed by centrifugation at $3000 \times g$ for 4 min at 4°C. The supernatant was then centrifuged at $75\,000 \times g$ for 30 min at 4°C. The resulting pellet of thylakoid membranes was resuspended in solubilization buffer containing 2 M urea, 7% SDS, 20% glycerol and 0.5 M Tris-HCl, pH 6.8, transferred in Eppendorf tubes, and centrifuged at $50\,000 \times g$ for 5 min to remove unsolubilized material. Chlorophyll concentration was measured by the method of [36], and samples were diluted with solubilization buffer to the final concentration of 200 nmol Chl/ml. Beta-mercaptoethanol was then added to a final concentration of 10%. Samples were stored at −80°C until ready for further processing.

2.3. SDS-PAGE and Western blot analysis

Thylakoid membrane proteins were resolved by SDS-PAGE using the discontinuous buffer system of [37] containing 12.5% acrylamide, 0.41% bis-acrylamide and 4 M urea. The stacking gel contained 4.5% acrylamide and 4 M urea. Gel lanes were loaded with 2–4 nmol Chl $(a + b)$. Electrophoresis on $0.15 \times 14 \times 16$ cm slab gels was performed at 2°C at a constant current of 8 mA for 16–18 h. Gels were stained with 0.1% Coomassie Brilliant Blue R for protein visualization, or incubated in transfer buffer for 30 min. Following resolution by SDS-PAGE, thylakoid membrane polypeptides were electrophoretically transferred onto a nitrocellulose membrane (Schleicher and Schuell, 0.1 μm) as described [38]. Immunochemical detection of the 32 and 34 kDa reaction center proteins of PS II was performed upon incubation with specific polyclonal antibodies raised in rabbit in this laboratory. Color development with alkaline-phosphatase conjugated antibodies was performed as described previously [15]. Immune cross reactions were quantitated by scanning the nitrocellu-

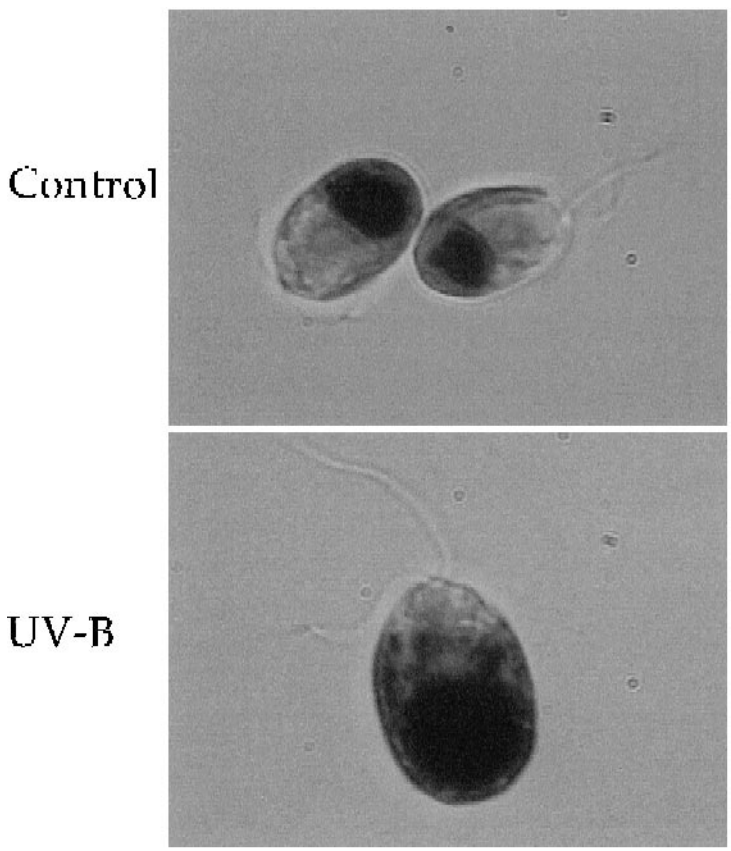

Fig. 1. Light microscope photographs of *Dunaliella salina* grown under PAR (Control, upper panel) or supplemental UV-B radiation (UV-B, lower panel). Note the significant difference in cell size upon growth under the two irradiance conditions. Magnification: 3200 ×.

lose membranes with a LKB-Pharmacia XL laser densitometer.

3. Results

3.1. Cell characteristics and rates of growth

D. salina cells are ellipsoid or ovate in shape and have a clearly polar structure, with two anterior flagellae, a single basal cup-shaped chloroplast that may partially surround the nucleus, and a distinctive mucilaginous cell coating. One macroscopic effect that was consistently observed in *D. salina* cultures grown under supplemental UV-B radiation was a significantly increased cell size. Fig. 1 shows *D. salina* photographs of control (upper panel) and UV-B-treated cells (lower panel), the latter being clearly larger than the control. Table 1 shows statistically significant differences in the dimension of cells grown under control or UV-B conditions. Both length and width were on the average 20% greater in UV-B-treated than control cells. On first approximation, a *D. salina* cell may be considered to be a rotational ellipsoid. As such, its volume can be calculated on the basis of the actual cell dimensions. Table 1 shows that the volume of UV-B-treated cells was about 108% greater than that of the control cells. In order to independently test this finding, 400 ml of *D. salina* cultures, containing a known number of cells, were precipitated in a packed cell volume (hematocrit) tube. The volume of the pellet from the UV-B grown sample was again about twice that of the control (Table 1). These results show that, in effect, the supplemental UV-B radiation under our growth conditions caused a doubling in the *D. salina* cell volume. Kinetically, cell dimensions and volume increased gradually upon transfer of control cultures to supplemental UV-B radiation, accompanied by an increase in the chlorophyll content of the cells (data not shown).

Table 1
Cell dimensions in control and UV-B-treated *D. salina*

Parameter measured	Control cells	UV-B-treated cells	Percentage change
Length (μm)	9.60	11.46	19.4
Width (μm)	6.44	7.86	22.0
Length/width ratio	3.46	3.91	13.0
Calculated cell volume (μm^3)	202	420	108
Packed cell volume (μm^3)	203	410	102

Cellular width and length dimensions were measured with a compound (light) microscope. Calculated cell volumes were based on the assumption of ellipsoid cell shape and were obtained upon application of the formula $V = \pi w^2 l/6$, where w is the ellipsoid width (cell diameter along the short axis) and l the ellipsoid length (cell diameter along the long axis). Packed cell volume was measured upon precipitation of a known number of cells in hematocrit tubes. Numbers are the mean value of at least 20 independent measurements. Standard error of the mean was about ±15% of the values given.

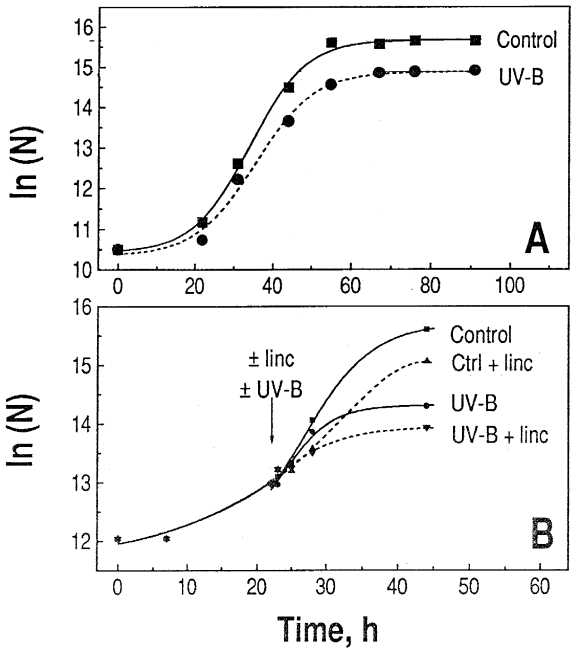

Fig. 2. Growth curves of *Dunaliella salina*. Plotted is the natural logarithm (ln) of the cell density per unit volume (*N* cells per ml) as a function of time after culture inoculation. A: growth under PAR (Control) or supplemental UV-B radiation (UV-B). B: effect of lincomycin on cell growth under PAR (Control) or supplemental UV-B conditions (UV-B).

Fig. 2A shows growth curves of *D. salina* cultivated under conditions of photosynthetic irradiance only (Control) or under supplemental UV-B-radiation. Plotted is the logarithm of the cell number as a function of time after culture inoculation. Following a commonly observed lag phase, which corresponds to adjustment of the cells in the fresh growth medium, the growth curves of control and UV-B-treated cells showed the following two significant differences.

(i) The cell density at the stationary phase (ln $N = 15.7$ for the control and ln $N = 14.9$ for the UV-B grown cells) suggests a difference by a factor of about two in the cell number per unit volume between control and UV-B-treated ($N = 6.6 \cdot 10^6$ cells/ml in the control versus $N = 3.0 \cdot 10^6$ cells/ml in the UV-B-treated culture). This difference in cell count might suggest that one or more nutrients in the growth medium become limiting earlier in the UV-B-treated than in the control culture. However, if the total biomass is calculated by normalisation of the number of cells with a factor that takes into account the cell volume, then the observed growth differences appear to be much less pronounced ($N_{\text{control}} \cdot Vol_{\text{control}} = \sim N_{\text{UV-B}} \cdot Vol_{\text{UV-B}}$).

(ii) The slope S of the logarithmic linear portion of the growth curve was consistently less steep in UV-B-treated cells, being $S_{\text{control}} = 0.15\ \text{h}^{-1}$ and $S_{\text{UV-B}} = 0.13\ \text{h}^{-1}$. This indicates a somewhat slower rate of cell division in the UV-B-treated than in the control samples.

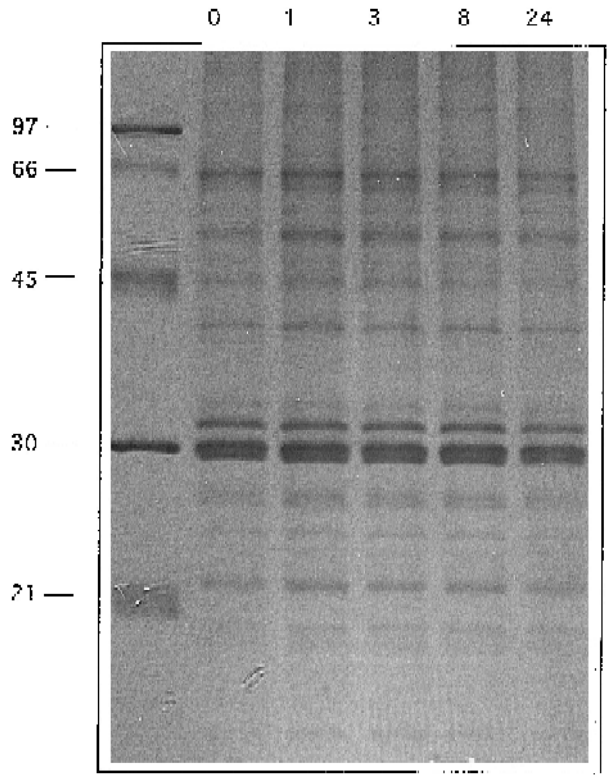

Fig. 3. SDS-PAGE profile of Coomassie-stained thylakoid membrane polypeptides of *D. salina* grown under PAR-conditions and exposed to supplemental UV-B radiation for variable periods of time. Lanes were loaded with 4 nmol chlorophyll.

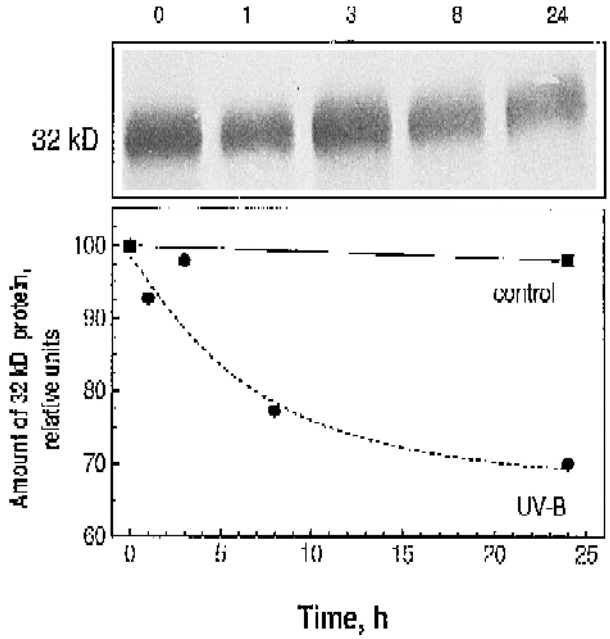

Fig. 4. Upper panel: Western blot analysis of *D. salina* thylakoid membrane polypeptides probed with specific polyclonal antibodies raised against the 32 kDa (D1) reaction center protein. Note the declining levels of D1 as a function of cell exposure to supplemental UV-B radiation. Lower panel: densitometric quantitation of the Western blot shown in the upper panel. Results were normalized on the amount of D1 present at zero time.

Fig. 2B shows changes in the growth of *D. salina* that occur upon transferring control cultures to supplemental UV-B conditions, in the presence or absence of the chloroplast protein biosynthesis inhibitor lincomycin. Following the transfer of control cells to supplemental UV-B, the rate of cell growth in the culture was lowered and the stationary phase was reached at a lower cell density. Addition of 1.5 mM lincomycin to the growth medium did not completely stop cell growth until a few hours after the addition of the antibiotic. During this period, it is expected that cell division and most of the metabolic processes would continue to occur, presumably by the enzymes already existing in the cell. However, 48 h after the addition of lincomycin, no viable cells could be detected in the growth medium. A 5-times higher concentration of this antibiotic yielded essentially the same results (data not shown), suggesting that lincomycin permeability into the cell is not a complicating factor in this phenomenology. The transfer of

control *D. salina* cultures to supplemental UV-B conditions was generally adverse to growth and this effect could be detected after a few hours under UV-B light. Addition of lincomycin to UV-B-treated cells also caused cell growth to stop within a few hours after the addition of this inhibitor. The extent of the inhibitory effect of lincomycin on cell growth was similar in control and UV-B-treated cells (Fig. 2B).

3.2. SDS-PAGE and Western blot analysis

Exposure of *D. salina* cultures to supplemental UV-B radiation did not change the profile of Coomassie stained-gels loaded with thylakoid membrane proteins (Fig. 3). Absence of significant changes in the polypeptide pattern over the 24-h UV-B exposure period eliminates the possibility of UV-B-induced gross changes in the protein composition of thylakoid membranes (Fig. 3). Fig. 4 (upper panel) shows a Western blot analysis of thylakoid membrane proteins probed with specific polyclonal antibodies against the 32 kDa (D1) reaction center protein of PS II. As evident in Fig. 4 (upper panel), a loss of cross reacting material at ~32 kDa occurs as a function of time under supplemental UV-B radiation; this decline is attributed to a specific UV-B-induced photodamage and loss of the D1 reaction center protein [30]. The D1 decay was quantitated by scanning nitrocellulose filters with a laser densitometer. Fig. 4 (lower panel) shows a loss of protein in this band by about 20% after 8 h and by about 30% over a 24 h period. A similar phenomenology was observed for the 34 kDa (D2) reaction center protein of PS II (Fig. 5).

Fig. 6 shows a Coomassie-stained gel loaded with thylakoid membrane protein from *D. salina* cells grown under PAR light only (control), and incubated in the presence of 1.5 mM lincomycin. The antibiotic did not affect either the pattern or intensity of the protein bands seen in the gel. However, when *D. salina* cells were exposed to supplemental UV-B radiation in the presence of lincomycin, loss of the diffuse protein bands from the 32–34 kDa region was evident in the Coomassie stained protein gel (Fig. 7).

Western blot analyses with specific polyclonal antibodies raised against the 32 kDa (D1) protein (Fig. 8) showed that indeed supplemental UV-B radiation

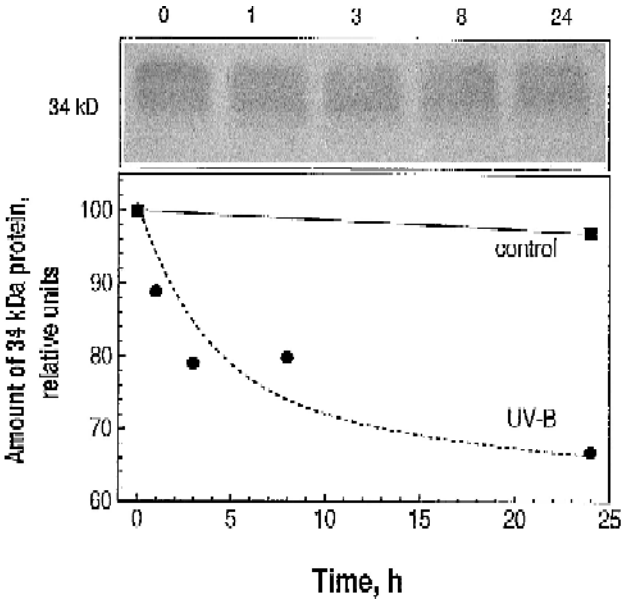

Fig. 5. Upper panel: Western blot analysis of *D. salina* thylakoid membrane polypeptides probed with specific polyclonal antibodies raised against the 34 kDa (D2) reaction center protein. Note the declining levels of D2 as a function of cell exposure to supplemental UV-B radiation. Lower panel: densitometric quantitation of the Western blots shown in the upper panel. Results were normalized on the amount of D2 present at zero time.

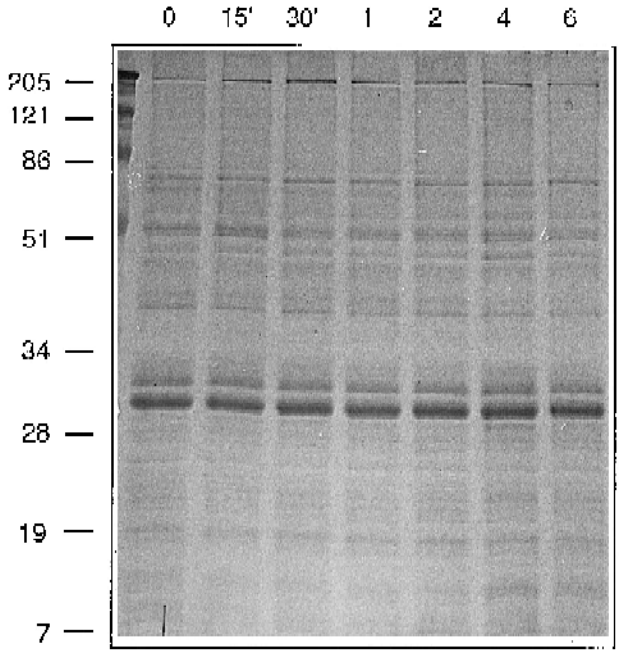

Fig. 6. SDS-PAGE profile of Coomassie-stained thylakoid membrane polypeptides of *D. salina* grown under PAR-conditions and incubated in the presence of 1.5 mM lincomycin. Lanes were loaded with 4 nmol chlorophyll.

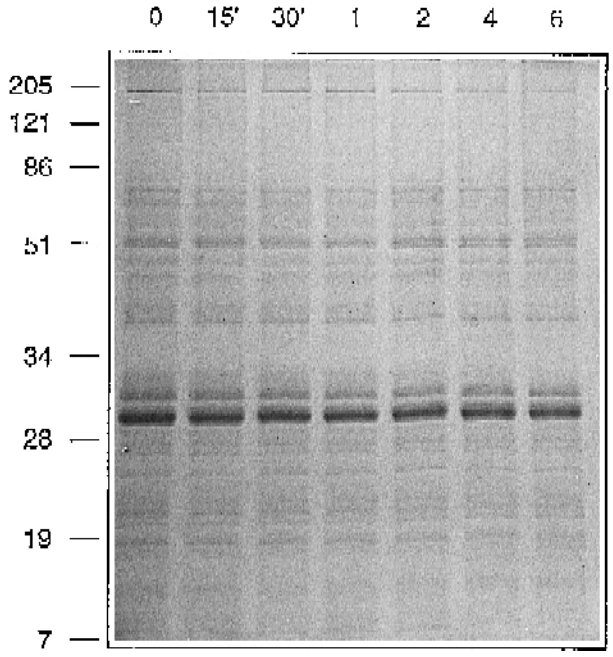

Fig. 7. SDS-PAGE profile of Coomassie-stained thylakoid membrane polypeptides of *D. salina* grown under supplemental UV-B radiation conditions and incubated in the presence of 1.5 mM lincomycin. Note the loss of stain from the 32–34 kDa region. Lanes were loaded with 4 nmol chlorophyll.

accelerated the loss of the D1 protein. The difference in the rate of D1 loss between UV-B + Lincomycin (Fig. 8, circles) over that in the presence of lincomycin only (Fig. 8, squares) is attributed to PS II photodamage brought about exclusively by the UV-B radiation. A similar acceleration in the loss of the 34 kDa (D2) protein was also observed in Western blot analyses, obtained with polyclonal antibodies specific for the D2 reaction center protein of PS II (Fig. 9).

Measurement of the half-lives of D1 and D2 revealed that both the 32 and 34 kDa proteins show a $t_{1/2} = 3.5–4$ h in the presence of lincomycin when cells are incubated strictly under PAR conditions. The half-lives of the two proteins were shortened significantly upon incubation in the presence of lincomycin under supplemental UV-B radiation ($t_{1/2} =$ 1.5–2 h, Figs. 8 and 9).

Recent work from this laboratory suggested that PAR photodamage and disassembly of the PS II holocomplex is promptly followed by formation of a 160 kDa protein complex in the thylakoid membrane of *D. salina*. This 160 kDa complex contained the photodamaged but as yet undegraded D1 protein [39] as well as the D2 protein of the PS II reaction center [40]. It was postulated that formation of such a 160 kDa protein complex might be an obligatory step in the PS II repair process of *D. salina*, designed to protect the D1/D2 heterodimer until degradation and replacement of the photodamaged protein could safely take place [41]. Thus, it was of interest to investigate whether formation of such complex is of significance in the case of PS II photodamage by supplemental UV-B radiation. Fig. 10 (upper panels) show the cross reaction between polyclonal antibodies and the 160 kDa complex in Western blots of control and UV-B-treated *D. salina*. In this experiment, 1.5 mM lincomycin were added to the growth medium at zero time. Fig. 10 (lower panel) presents a quantitation of

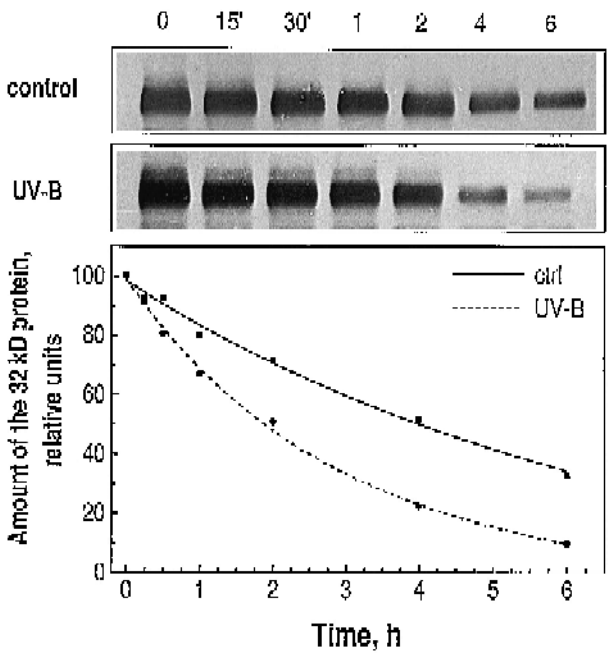

Fig. 8. Upper panels: Western blot analysis of *D. salina* thylakoid membrane polypeptides probed with specific polyclonal antibodies raised against the 32 kDa (D1) reaction center protein. Cells were grown under PAR (control) or supplemental UV-B radiation (UV-B). Addition of lincomycin to the cultures (1.5 mM final concentration) occurred at zero time. Note the declining levels of D1 as a function of lincomycin incubation. Lower panel: densitometric quantitation of the Western blots shown in the upper panels. Results were normalized on the amount of D1 present at zero time. Note the faster loss of D1 under supplemental UV-B than PAR conditions.

the relative abundance of the 160 kDa complex as a function of time after addition of lincomycin.

Addition of lincomycin to the control culture caused a transient increase by about 60% in the steady-state amount of the 160 kDa complex. This increase lasted for up to 2 h, after which the abundance of this complex in the thylakoid membranes started to decline (Fig. 10, lower panel, squares). This finding is consistent with earlier measurements performed in the presence of chloramphenicol, another chloroplast protein biosynthesis inhibitor [39]. In samples exposed to supplemental UV-B radiation, the abundance of the 160 kDa protein complex did not show a transient increase following addition of lincomycin to the culture. Rather, a decline in the intensity of the 160 kDa protein band was observed promptly upon addition of the protein biosynthesis inhibitor (Fig. 10, lower panel, circles). The half-time for the loss of the 160 kDa complex under supplemental UV-B and lincomycin conditions was about 2 h, i.e., similar to that of D1 and D2 under the same conditions (Figs. 8 and 9).

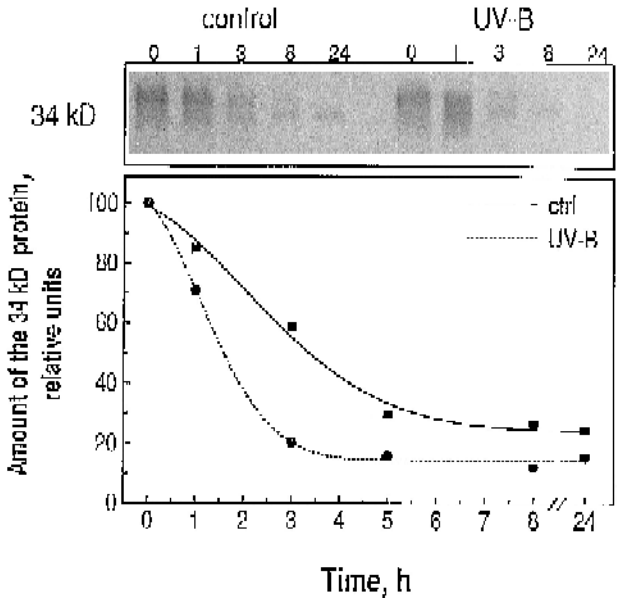

Fig. 9. Upper panel:Western blot analysis of *D. salina* thylakoid membrane polypeptides probed with specific polyclonal antibodies raised against the 34 kDa (D2) reaction center protein. Cells were grown under PAR (control) or supplemental UV-B radiation (UV-B). Addition of lincomycin to the cultures (1.5 mM final concentration) occurred at zero time. Note the declining levels of D2 as a function of lincomycin incubation. Lower panel: densitometric quantitation of the Western blots shown in the upper panel. Results were normalized on the amount of D2 present at zero time. Note the faster loss of D2 under supplemental UV-B than PAR conditions.

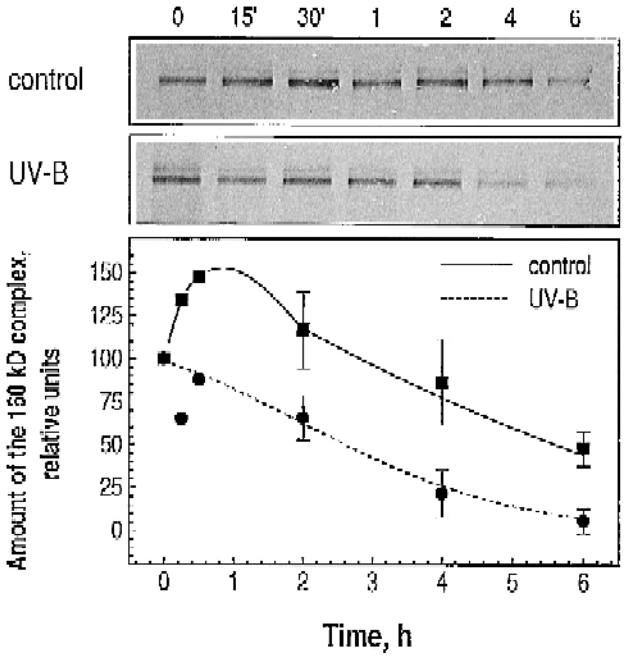

Fig. 10. Western blot analysis of *D. salina* thylakoid membrane proteins migrating to the 160 kDa region. Cells were grown under PAR (control) or supplemental UV-B radiation (UV-B). Addition of lincomycin to the cultures (1.5 mM final concentration) occurred at zero time. Upper panels: cross reaction between D1 polyclonal antibody and the 160 kDa protein complex in cells grown under PAR (control) or supplemental UV-B radiation (UV-B). Lower panel: densitometric quantitation of the Western blots shown in the upper panels. Results were normalized on the amount of the 160 kDa complex present at zero time. Note the transient accumulation of the 160 kDa complex in the PAR control and the prompt decline in the amount of this complex under supplemental UV-B conditions.

4. Discussion

In contrast to photoinhibition by visible light, where photodamage is mediated by chlorophyll [18,30,42], the primary sites of damage by supplemental UV-B radiation are the specialised bound quinone Q_A and Q_B of PS II and the plastoquinone pool [31]. Consistent with this view is the observation that inhibitors that displace plastoquinone were found to inhibit UV-B-induced D1 degradation [34]. This

view has recently been challenged, however. Instead, tyrosine residues and the Mn cluster in the water-oxidising complex have been implicated [33,43]. Irrespective of the mechanism, earlier and recent studies demonstrate the sensitivity of PS II to UV-B radiation and emphasise the UV-B-induced inhibition in the water-to-plastoquinone oxidoreductase function which results in slower rates of photosynthesis and cell growth [44]. Moreover, a UV-B-induced inhibition in the function of the carboxylating enzyme Rubisco would further compound this adverse effect [26,27]. To better understand the cellular responses to supplemental UV-B, we undertook to investigate the effect of such radiation at the cellular and thylakoid membrane levels.

4.1. Effect of supplemental UV-B on cell morphology

The data on *D. salina* growth (Fig. 1 and Table 1) show that UV-B-treated cells undergo changes in morphology, primarily consisting of an increase in cell size. Cell volume estimates were obtained independently from the cell dimensions, as measured via a light microscope (Fig. 1), and from the packed cell volume of a known cell number. These measurements showed a doubling of the *D. salina* cell volume under supplemental UV-B, consistent with similar results observed in UV-B-treated *Chlorella vulgaris* where cell volume increase was accompanied by an increase in starch content [45]. Such changes in cell size can be seen as a response or adaptation to the UV-B. The lower cell surface/volume ratio may be effective in countering oxidative damage, with the cell wall and the other membranes probably acting as shields [46]. Inconsistent with this view, however, is the observation that UV-B treatment of chloroplasts in vivo or *in organello* resulted in a similar extent of impairment of photosynthesis [45]. Further, dinoflagellates of distinctly different cell size were equally susceptible to UV-B radiation [47].

A more likely explanation of the UV-B-induced cell size increase is that such radiation causes damage to cellular DNA, leading to the formation of pyrimidine dimers and other photoproducts [48] which in effect interfere with the cell cycle. In particular, specific retardation of the cell cycle in the S phase may be attributed to on-going DNA repair under UV-B while such retardation in the G2 phase may be related to UV-B-induced damage of microtubules [49]. In UV-B-treated diatoms, cell enlargement occurred without a concomitant cell division [46]. Thus, cells were capable of growth under conditions where one, or more, steps in the progression of the cell cycle were impaired. In essence, this response is similar to that of other ionizing radiations [50], known to cause DNA damage and cell cycle arrest in yeast and mammalian cells, with the inhibition usually occurring in the G2 phase [51].

Interestingly, the total biomass in the fully contained *D. salina* cultures, calculated as $N_{\text{cells}} \cdot Vol_{\text{cells}}$, was unaffected under the experimental conditions employed in this work, suggesting that in spite of the UV-B-induced photodamage and impairment, cells were able to utilise, albeit more slowly, the entire nutrient supply of the culture medium and, through photosynthesis, to accumulate biomass equivalent to that observed under PAR conditions.

Water does not absorb UV-B radiation, however, dissolved organic and inorganic matter may screen and significantly attenuate this radiation in nature. Moreover, it has been observed that motile cells of the phytoplankton often respond to UV-B radiation by negative phototaxis, i.e., moving away from the surface into deeper areas of the culture medium where the UV-B intensity is lower [52,53]. Thus, extrapolation of the findings in this work to growth in marine and freshwater ecosystems may be complicated due to great changes in spectral irradiance, vertical mixing and vertical migration of cells in the water column. Complications may also arise because of variable UV-B/UV-A/PAR ratios [54] and due to the general lack of information on species-specific responses to UV-B exposure [55]. Changes in cell size, as reported in this work, are likely to occur in Antarctic phytoplankton communities, as these are primary targets of enhanced UV-B [27,46]. The above considerations should therefore be taken into account when attempting to arrive at predictions on marine phytoplankton productivity in relationship to stratospheric ozone depletion in ecologically sensitive areas of the globe.

4.2. Effects of supplemental UV-B on Photosystem II

This work further shows that transitions from PAR-only to PAR + UV-B during cell growth cause

a lowering in the steady-state amount of both D1 and D2 proteins with similar rates. Under our experimental conditions, a 24 h exposure of *D. salina* to supplemental UV-B radiation caused a lowering of D1 and D2 to 60–65% of that found in the PAR control (Figs. 4 and 5). Thus, under supplemental UV-B radiation, *D. salina* cells operate with a smaller number (by ~30–35%) of PS II reaction centres than control cells. This steady-state probably reflects a condition where the rate of PAR-induced and UV-B-induced photodamage begins to approach the rate limiting step of the overall repair.

The enhanced rates of D1 and D2 photodamage under supplemental UV-B radiation were confirmed with measurements conducted in the presence of lincomycin, a chloroplast protein biosynthesis inhibitor that blocks the de novo biosynthesis of D1 and D2 (Figs. 8 and 9). It should be noted, however, that distinctly different repair pathways must occur following photodamage by PAR versus that occurring under supplemental UV-B.

Under PAR, only the D1 protein is subject to photodamage [23,56]. The apparent loss of the 32 and 34 kDa forms of D1 and D2, respectively (Figs. 8 and 9, squares), may be attributed to the fact that the repair process from PAR-induced photodamage involves the prompt disassembly of the PS II holocomplex and the conversion of the D1/D2 heterodimer into a 160 kDa holding complex ([39,41], see also the squares in Fig. 10).

Under supplemental UV-B, both D1 and D2 proteins are subject to photodamage [31,34,57,58]. In this case, however, the loss of the 32 and 34 kDa forms of D1 and D2, respectively (Figs. 8 and 9, circles), cannot be attributed to the conversion of the D1/D2 heterodimer into a 160 kDa holding complex. Indeed, under supplemental UV-B, the 160 kDa complex itself decays with a half-life similar to that of D2 (Fig. 10, circles). These results suggest that significantly different pathways operate for the repair of PS II from photodamage under PAR and supplemental UV-B. It is evident that, in the case of supplemental UV-B, photodamage and repair of D2 is as central a process as that for D1 under PAR [31,34].

D. salina grown under supplemental UV-B may possess a unique enzymatic process for the repair of PS II from UV-B photodamage. Ultraviolet-B radiation is known to induce specific gene expression of genes involved in defence and repair processes [59]. Thus, it is possible that D1 and/or D2 degradation and replacement under supplemental UV-B involves the induction of specific genes coding for proteins that are dedicated to operate under UV-B conditions. Such consideration will explain the differential response of the 160 kDa complex under PAR versus UV-B conditions. Accumulation of the 160 kDa complex occurs only under PAR (Fig. 10, squares), presumably because processing of photodamaged D1 requires de novo protein biosynthesis. Degradation and loss of both D1 and D2 occurs under supplemental UV-B (Fig. 10, circles) as the targets of photodamage and proteolysis are different under these conditions [31,32,57].

Acknowledgements

The work was supported by USDA NRICGP 96-35100-3201 Grant to A. Melis. Support by the UC Education Abroad Program to A. Masi is gratefully acknowledged.

References

[1] J. Myers, J.R. Graham, R.T. Wang, Plant Physiol. 66 (1980) 1144–1149.
[2] Y. Fujita, K. Ohki, A. Murakami, Plant Cell Physiol. 26 (1985) 1541–1548.
[3] A. Manodori, A. Melis, Plant Physiol. 82 (1986) 185–189.
[4] F.X. Cunningham, R.J. Dennenberg, P.A. Jursinic, E. Gantt, Plant Physiol. 93 (1990) 888–895.
[5] S. Abe, A. Murakami, K. Ohki, Y. Aruga, Y. Fujita, Plant Cell Physiol. 35 (1994) 901–906.
[6] A. Melis, A. Murakami, J.A. Nemson, K. Aizawa, K. Ohki, Y. Fujita, Photosynth. Res. 47 (1996) 253–265.
[7] A. Melis, G.W. Harvey, Biochim. Biophys. Acta 637 (1981) 138–145.
[8] J.M. Anderson, W.S. Chow, H. Adamson, A. Melis, in: J.H. Argyroudi-Akoyunoglou (Ed.), Regulation of Chloroplast Biogenesis NATO ASI Series A: Life Sciences, vol. 226, Plenum Press, New York, 1992, pp. 483–490.
[9] J.H. Kim, R.E. Glick, A. Melis, Plant Physiol. 102 (1993) 181–190.
[10] J.M. Anderson, Annu. Rev. Plant Physiol. 37 (1986) 93–136.
[11] A. Melis, Biochim. Biophys. Acta 1058 (1991) 87–106.
[12] T.A. Leong, J.M. Anderson, Photosynth. Res. 5 (1984) 105–115.

[13] U.K. Larsson, J.M. Anderson, B. Andersson, Biochim. Biophys. Acta 894 (1987) 69–75.
[14] A. Sukenik, J. Bennett, P.G. Falkowski, Biochim. Biophys. Acta 932 (1988) 206–215.
[15] B.M. Smith, P.J. Morrissey, J.E. Guenther, J.A. Nemson, M.A. Harrison, J.F. Allen, A. Melis, Plant Physiol. 93 (1990) 1433–1440.
[16] S.B. Powles, Annu. Rev. Plant Physiol. 35 (1984) 15–44.
[17] R.E. Cleland, P.J. Neale, A. Melis, Photosynth. Res. 9 (1986) 79–88.
[18] S. Demeter, P.J. Neale, A. Melis, FEBS Lett. 214 (1987) 370–374.
[19] J. Barber, B. Andersson, Trends Biochem. Sci. 17 (1992) 61–66.
[20] I. Ohad, D.J. Kyle, C.J. Arntzen, J. Cell Biol. 99 (1984) 481–485.
[21] B.M. Greenberg, V. Gaba, A.K. Mattoo, M. Edelman, EMBO J. 6 (1987) 2865–2869.
[22] A. Mattoo, H. Hoffman-Falk, J. Marder, M. Edelman, Proc. Natl. Acad. Sci. USA 81 (1984) 1380–1384.
[23] A.K. Mattoo, M. Edelman, Proc. Natl. Acad. Sci. USA 84 (1987) 1497–1501.
[24] J.E. Guenther, A. Melis, Photosynth. Res. 23 (1990) 105–110.
[25] J.F. Bornman, J. Photochem. Photobiol. 4 (1989) 145–158.
[26] A. Strid, W.S. Chow, J.M. Anderson, Biochim. Biophys. Acta 1020 (1990) 260–268.
[27] P.J. Neale, J.J. Cullen, M.P. Lesser, A. Melis, in: H. Yamamoto, C.M. Smith (Eds.), Photosynthetic Responses to the Environment, American Society of Plant Physiology, Rockville, MD, 1993, pp. 61–77.
[28] Sisson, W.B. (1986) in: R.C. Worrest, M.M. Caldwell (Eds.), Stratospheric Ozone Reduction, Solar Ultraviolet Radiation and Plant Life, pp. 75–84.
[29] B.R. Jordan, in: J.A. Callow (Ed.), Advances in Botanical Research, Academic Press, London, 1996, pp. 97–162.
[30] B.M. Greenberg, V. Gaba, O. Canaani, S. Malkin, A.K. Mattoo, M. Edelman, Proc. Natl. Acad. Sci. USA 86 (1989) 6617–6620.
[31] A. Melis, J.A. Nemson, M.A. Harrison, Biochim. Biophys. Acta 1100 (1992) 312–320.
[32] G. Friso, R. Barbato, G.M. Giacometti, J. Barber, FEBS Lett. 339 (1994) 217–221.
[33] R. Barbato, A. Frizzo, G. Friso, F. Rigoni, G.M. Giacometti, Eur. J. Biochem. 227 (1995) 723–729.
[34] M.A.K. Jansen, B. Depka, A. Trebst, M. Edelman, J. Biol. Chem. 268 (1993) 21246–21252.
[35] U. Pick, L. Karni, M. Avron, Plant Physiol. 81 (1986) 92–96.
[36] D.I. Arnon, Plant Physiol. 24 (1949) 1–15.
[37] U. Laemmli, Nature 227 (1970) 680–685.
[38] H. Towbin, T. Staehelin, J. Gordon, Proc. Natl. Acad. Sci. USA 76 (1979) 4350–4354.
[39] J.H. Kim, J.A. Nemson, A. Melis, Plant Physiol. 103 (1993) 181–189.
[40] A. Melis, J. Nemson, Photosynth. Res. 46 (1995) 207–211.
[41] I. Baroli, A. Melis, Planta 198 (1996) 640–646.
[42] D. Bumann, D. Oesterhelt, Proc. Natl. Acad. Sci. USA 26 (1995) 12195–12199.
[43] C. Spetea, E. Hideg, I. Vass, Plant Sci. 115 (1996) 207–215.
[44] S. Nogués, N.R. Baker, Plant Cell Environ. 18 (1995) 781–787.
[45] G. Malanga, S. Puntarulo, Physiol. Plant. 94 (1995) 672–679.
[46] D. Karentz, J.E. Cleaver, D.L. Mitchell, J. Phycol. 27 (1991) 326–341.
[47] N.G.A. Ekelund, Physiol. Plant. 91 (1994) 696–702.
[48] A.B. Britt, Plant Physiol. 108 (1995) 891–896.
[49] T.G. Zaremba, T.R. LeBon, D.B. Millar, R.M. Smejkal, R.J. Hawley, Biochemistry 23 (1984) 1073–1080.
[50] D.E. Lea, Actions of Radiations on Living Cells, 2nd edn., Cambridge University Press, New York, 1955, 416 pp.
[51] T. Weinert, L. Hartwell, J. Cell Sci. (Suppl.) 12 (1989) 145–148.
[52] B. Eggersdorfer, D.P. Haeder, FEMS Microbiol. Ecol. Lett. 85 (1991) 319–326.
[53] C. Sebastian, R. Scheuerlein, D.P. Haeder, J. Exp. Mar. Biol. Ecol. 182 (1994) 251–263.
[54] R.C. Smith, S.B. Baker, Photochem. Photobiol. 29 (1979) 311–323.
[55] D. Karentz, J.E. Cleaver, D.L. Mitchell, Nature 350 (1991) 28.
[56] C. Vasilikiotis, A. Melis, Proc. Natl. Acad. Sci. USA 91 (1994) 7222–7226.
[57] G. Friso, C. Spetea, G.M. Giacometti, I. Vass, R. Barbato, Biochim. Biophys. Acta 1184 (1994) 78–84.
[58] I. Vass, L. Sass, C. Spetea, A. Bakou, D.F. Ghanotakis, V. Petrouleas, Biochemistry 35 (1996) 8964–8973.
[59] A. Strid, Plant Cell Physiol. 34 (1993) 949–953.